Gravity waves from the non-renormalizable Electroweak Vacua phase transition

Eric Greenwood

CERCA, Department of Physics, Case Western Reserve University, Cleveland, OH 44106-7079

Pascal M. Vaudrevange

CERCA, Department of Physics, Case Western Reserve University, Cleveland, OH 44106-7079 and
DESY, Notkestrasse 85, 22607 Hamburg, Germany

It is currently believed that the Standard Model is an effective low energy theory which in principle may contain higher dimensional non-renormalizable operators. These operators may modify the standard model Higgs potential in many ways, one of which being the appearance of a second vacuum. For a wide range of parameters, this new vacuum becomes the true vacuum. It is then assumed that our universe is currently sitting in the false vacuum. Thus the usual second-order electroweak phase transition at early times will be followed by a second, first-order phase transition. In cosmology, a first-order phase transition is associated with the production of gravity waves. In this paper we present an analysis of the production of gravitational waves during such a second electroweak phase transition. We find that, for one certain range of parameters, the stochastic background of gravitational waves generated by bubble nucleation and collision have an amplitude which is estimated to be of order $\Omega_{GW} h^2 \sim 10^{-11}$ at $f = 3 \times 10^{-4}$Hz, which is within reach of the planned sensitivity of LISA. For another range of parameters, we find that the amplitude is estimated to be of order $\Omega_{GW} h^2 \sim 10^{-25}$ around $f = 10^3$Hz, which is within reach of LIGO. Hence, it is possible to detect gravity waves from such a phase transition at two different detectors, with completely different amplitude and frequency ranges.

I. INTRODUCTION

Recently, the authors in [1] have analyzed the scalar field theory of a standard model Higgs field whose potential includes non-renormalizable operators up to mass dimension 8. In this model, a second true vacuum appears which may be responsible for the observed late-time acceleration of the universe. While the electroweak phase transition remains second order, the subsequent phase transition from the second false vacuum to the true vacuum is first order, giving rise to the possibility of bubble nucleation. In this picture, we are sitting in the second false vacuum (located e.g. around $\phi \approx 0.3$ TeV in Fig. 1), awaiting the plunge into the true vacuum (around $\phi \approx 0.8$ TeV). There are certain fore-bearers of this impending doom that are in principle observable.

In particular, it is well-known that bubble collisions lead to the production of gravitational waves (GW), due to the breaking of symmetry. The strength of the phase transition, as well as the amplitude of the GW are strongly model and parameter dependent. Thus it seems worthwhile to investigate whether this non-renormalizable Higgs model can have a background of interest for current and proposed GW detectors[1], specifically LIGO, Advanced LIGO, Geo 600, Virgo [2] and as well as the proposed LISA experiment [3].

---

[1] It should be pointed out that a possible detection of gravitational waves from bubble collisions of this phase transition would give us only a brief time before the joint bubble of true vacuum passes through us – the bubble wall moves at close to and gravitational waves move exactly at the speed of light.

The two main sources of GW production are the nucleation and collision of bubbles of true vacuum and the onset of turbulence. In this paper we shall restrict ourselves to the first case, that of collisions of bubbles of true vacuum. In order to tackle this problem, we rely on the pioneering work of [4, 5] who developed a semi-analytical model for the GW spectrum emitted from bubble collisions.

This paper is organized as follows. Section II briefly reviews the model proposed in [1]. In Section III, we review the thin-wall approximation of [4, 5]. In Section IV we present the results of our calculation. Finally, we conclude in Section V.

II. ELECTROWEAK MODEL

In [1] the authors considered the standard Higgs potential with additional higher order non-renormalizable terms. These non-renormalizable terms do not pose a problem as long as they are suppressed by small enough coupling constants, i.e. large enough masses. The potential considered is given by,

$$V(\phi) = -\frac{\mu^2}{2}\phi^2 + \frac{\lambda_1}{4}\phi^4 - \frac{\lambda_2}{8}\phi^6 + \frac{\lambda_3}{16}\phi^8 + V_0. \quad (1)$$

For later use, we rewrite the potential as

$$V(\phi) = -\varepsilon_0 \phi_1^3 \phi_2^3 \phi^2 + \frac{\lambda_3}{16}(\phi^2 - \phi_1^2)^2(\phi^2 - \phi_2^2)^2 + V_0', \quad (2)$$

with

$$\phi_1^2 \equiv \frac{2}{\lambda_3 \phi_2^2}\left(\lambda_1 - \frac{1}{4}\frac{\lambda_2^2}{\lambda_3}\right), \qquad (3)$$

$$\phi_2^2 \equiv \frac{1}{2}\frac{\lambda_2}{\lambda_3}\left(1 + \sqrt{3 - \frac{8\lambda_1\lambda_3}{\lambda_2^2}}\right), \qquad (4)$$

$$\varepsilon_0 \equiv \frac{\mu^2}{2\phi_1^3\phi_2^3} - \frac{\lambda_3}{8\lambda_1\lambda_2}(\phi_1^2 + \phi_2^2), \qquad (5)$$

$$V_0' \equiv V_0 - \frac{\lambda_3}{16}\phi_1^4\phi_2^4, \qquad (6)$$

In the latter form, the finite temperature effective potential formulation of the theory is more easily written down.

The parameter ε_0 assumes the role of a controllable fine tuning of the potential. When $\varepsilon_0 = 0$, the potential in Eq. (2) has four degenerate minima at $\phi = \pm\phi_1, \pm\phi_2$. When $\varepsilon_0 \neq 0$, the degeneracy of the vacua between $\phi = \phi_1, \phi_2$ ($\phi = -\phi_1, -\phi_2$) is broken and there is an energy difference between the energy densities of the two vacua, as shown in Fig. 1 (at $T = 0$). The difference in energy is given as

$$\delta V = \varepsilon_0 \phi_1^3 \phi_2^3 (\phi_2^2 - \phi_1^2), \qquad (7)$$

where $\phi_2 > \phi_1$.

Finite-temperature effects are approximated by adding a thermal mass term to the potential in Eq. (2), hence the potential takes the form $V(\phi, T) = cT^2\phi^2/2 + V(\phi, 0)$, where c is generated by the quadratic terms that acquire a ϕ-dependent mass in the high-temperature expansion of the one-loop thermal potential. In general there are also terms in the high-temperature thermal expansion that are proportional to $T^4\phi^4$. However, it was argued in [6] that these terms only lead to small corrections to the potential, therefore we shall ignore these contributions. In terms of the temperature, the effective potential then becomes

$$V(\phi, T) = -\varepsilon(T)\phi_1^3\phi_2^3\phi^2 + \frac{\lambda_3}{16}(\phi^2 - \phi_1^2)^2(\phi^2 - \phi_2^2)^2 + V_0', \qquad (8)$$

where

$$\varepsilon(T) = \varepsilon_0 - \frac{cT^2}{\phi_1^3\phi_2^3}. \qquad (9)$$

Using the procedure outlined in [7, 8], the constant c is found to be given by

$$c = \frac{1}{16}(3g^2 + g'^2 + 4y_t^2 + \frac{1}{32}\lambda_1) \qquad (10)$$

where g and g' are the $SU(2)_L$ and $U(1)_Y$ gauge couplings, and y_t is the top Yukawa coupling. Using the excepted values of these couplings and that the Higgs mass is 0.08 TeV $< m_H < 0.15$ TeV, one finds that from Eq. (10), $c \approx 1.7$. The critical temperature is defined when $\varepsilon(T) = 0$ is zero or in other words

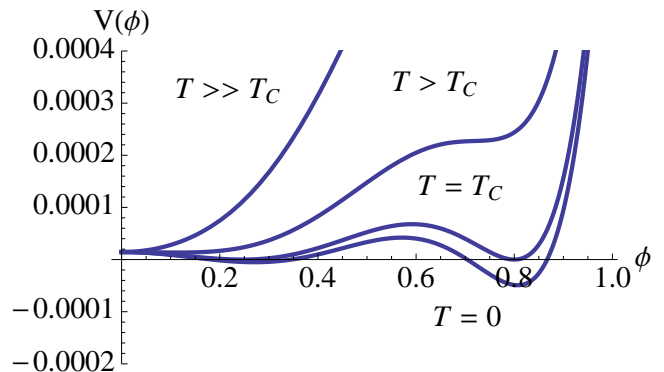$$T_c^2 = \frac{\varepsilon_0\phi_1^3\phi_2^3}{c}. \qquad (11)$$

FIG. 1: The temperature dependence of the ϕ^8 Higgs field potential given in Eq. (8). The values used in this plot are $\phi_1 = 0.246$ TeV, $\phi_2 = 0.8$ TeV, $\lambda_3 = 0.154$ TeV^{-4}, $V_0' = 0$ and $\varepsilon_0 = 0.01$ TeV^{-4}.

In this case, the vacua are degenerate, as discussed above.

In Fig. 1 we plot the temperature dependence of the potential in Eq. (8). Since the potential is symmetric for $\phi \to -\phi$, we will consider only the $\phi > 0$ half-plane. For very high temperatures ($T >> T_c$), the quadratic term of the potential dominates and the potential consists of a characteristic "U" shape with a single minimum at $\phi = 0$. Here, the Higgs field has zero expectation value and the electroweak symmetry is left unbroken. As T decreases, $\phi = 0$ becomes a maximum ($T > T_c$) and the field begins to roll down the potential toward the first minimum, which is forming at $\phi = \phi_1$. The second minimum is forming at $\phi = \phi_2$ at higher energy, making it non-accessible since it is a less favorable state. The non-zero expectation value of the Higgs field at $\phi = \phi_1$ breaks the electroweak symmetry. This is the standard picture of electroweak symmetry breaking from a field going through a second order phase transition. However, the Higgs potential keeps evolving as the temperature decreases. The the second minimum at $\phi = \phi_2$ drops to lower energies until it becomes the true global minimum after the temperature falls below T_c, causing the minimum at $\phi = \phi_1$ to be the false minimum. In other words, the Higgs field sitting there in the false vacuum can undergo a first order phase transition by tunneling to the global minimum at $\phi = \phi_2$ and forming bubbles of true vacuum.

As is well known, both nucleation of bubbles and their collisions can source gravitational waves. In the next section we will review the production of gravitational waves via bubble collision.

III. GRAVITATIONAL WAVE PRODUCTION IN PHASE TRANSITIONS

We are interested in production of gravitational waves from a first-order phase transition of the Higgs field. The

Lagrangian for the Higgs field φ is given by

$$L = \frac{1}{2}\partial^\mu\varphi\partial_\mu\varphi - V(\varphi), \qquad (12)$$

where the potential possesses at least two non-degenerate local minima, such as that in Eq. (2) (as shown in Fig. 1). In the following, we use a metric with signature $(+---)$. Classically, the false vacuum state is stable: a field sitting in this vacuum will remain there forever. However, quantum effects can cause the false vacuum to decay to the true vacuum. This decay proceeds via the nucleation and expansion of bubbles of true vacuum, which spontaneously appear in the false vacuum. The bubbles then expand due to the energy difference between the two vacua, which induces an effective pressure on the bubble wall. This causes a bubble to expand with an initial acceleration, with its expansion speed quickly approaching the speed of light.

In [9], Coleman showed that the bubble evolves according to a Klein-Gordon equation with $O(3,1)$ symmetry which implies that the position of the bubble wall is given by

$$\vec{x}_{wall}^2 - t^2 = R_0^2, \qquad (13)$$

where R_0 is the initial radius of the bubble and $\vec{x}_{wall}$ denotes a fiducial point with in the bubble wall. When t is sufficiently large, we see that the position of the bubble wall is given by $R(t) \approx t$, hence the radius of the bubble wall is proportional to the elapsed time. From Eq. (12), the stress-energy tensor associated with the bubble is

$$T_{\mu\nu}(\vec{x},t) = \partial_\mu\varphi\partial_\nu\varphi - g_{\mu\nu}L \qquad (14)$$

where the energy density of the bubble is the T_{00} component.

To determine the gravity-wave production we shall employ the envelope approximation, originally developed by [10] in the context of the linearized gravity approximation. This approximation is valid for bubble sizes less than H^{-1}. The energy radiated in gravitational waves is given by the Fourier transform of the spatial components of the stress-energy tensor in Eq. (14). Here, we will neglect the $g_{\mu\nu}L$ term, since it is a pure trace term and does not contribute to the production of the gravitational waves. Following Weinberg [11], the Fourier transform can be shown to be

$$T_{ij}(\hat{\vec{k}},\omega) = \frac{1}{2\pi}\int_0^\infty dt\, e^{i\omega t}\int d\vec{x}\,\partial_i\varphi\partial_j\varphi\, e^{-i\omega\hat{\vec{k}}\cdot\vec{x}}, \quad (15)$$

where $\hat{\vec{k}}$ is a unit wave vector. In the envelope approximation, one assumes that the regions that have overlapped do not contribute substantially to the gravitational radiation. Thus, these regions are excluded from the spatial integrals. Assuming that the time of nucleation for the

bubbles is $t = 0$, [10] showed that Eq. (15) leads to

$$T_{ij}(\hat{\vec{k}},\omega) = \frac{\rho_{vac}}{6\pi}\int_0^\infty dt\, e^{i\omega t}\sum_{n=1}^N t^3 e^{-i\omega\hat{\vec{k}}\cdot\vec{k}_n} \times$$
$$\int_{S_n} d\Omega e^{-i\omega\hat{\vec{k}}\cdot\vec{k}}\hat{\vec{k}}_i\hat{\vec{k}}_j \quad (16)$$

where the sum is over the number of colliding bubbles. From Weinberg, the total energy radiated in gravity waves is given as

$$\frac{dE}{d\omega d\Omega} = 2G\omega^2\Lambda_{ij,lm}(\hat{\vec{k}})T_{ij}^*(\vec{k},\omega)T_{lm}(\vec{k},\omega) \qquad (17)$$

where $\Lambda_{ij,lm}$ is the projection tensor for gravity waves:

$$\Lambda_{ij,lm}(\hat{\vec{k}}) = \delta_{il}\delta_{jm} - 2\hat{\vec{k}}_j\hat{\vec{k}}_m\delta_{il} + \frac{1}{2}\hat{\vec{k}}_i\hat{\vec{k}}_j\hat{\vec{k}}_l\hat{\vec{k}}_m$$
$$- \frac{1}{2}\delta_{ij}\delta_{lm} + \frac{1}{2}\delta_{ij}\hat{\vec{k}}_l\hat{\vec{k}}_m + \frac{1}{2}\delta_{lm}\hat{\vec{k}}_i\hat{\vec{k}}_j. \qquad (18)$$

To compare our results with those found in [10], we compute the case of two-bubbles colliding in the linearized gravity approximation. In Figs. 2 and 3 we plot some of our numerical results. Here d is the initial distance between the two-bubbles. To simplify notation, we are plotting in units of $G\rho_{vac}/3$ which is just a constant, thus the relative magnitude of the curves in Figs. 2 and 3 will be reduced. In Fig. 2 we plot the scaled energy spectrum for initial separation of $d = 60$, while in Fig. 3 we plot the scaled energy spectrum per octave frequency interval. Comparing our results, we see that the results are qualitatively the same, hence consistent with those in [10]. This is expected since we are using the envelope method, where the only dependence on the specific models potential comes in the form of ρ_{vac}, which is just a constant.
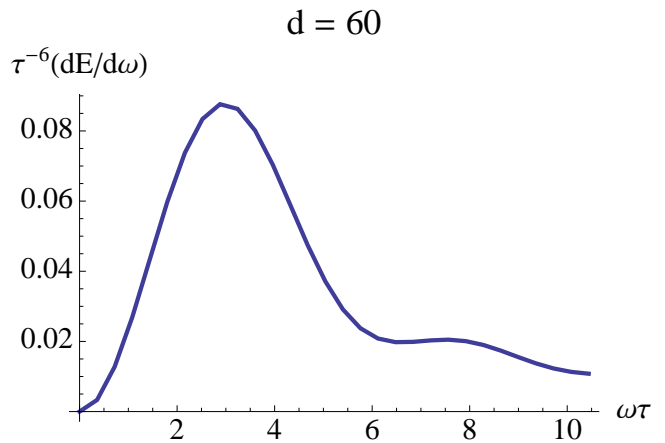

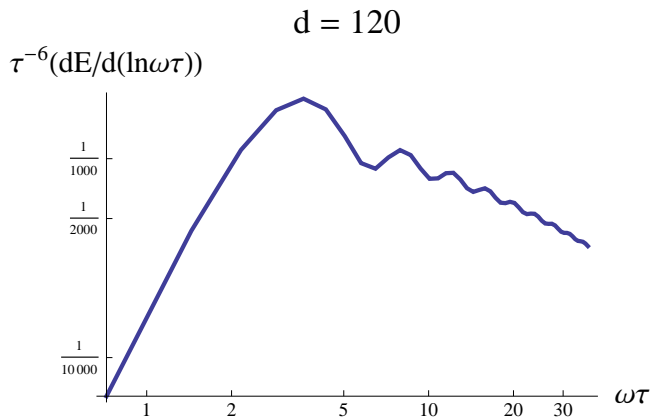FIG. 2: Scaled energy spectrum for initial bubble separation of $d = 60$.

d = 120

FIG. 3: Scaled energy spectrum per octave frequency interval.

IV. GRAVITATIONAL WAVE PARAMETERS

To estimate the spectrum of gravitational waves that are sourced by this phase transition, we need to estimate the tunneling rate for the decay of the false vacuum state to the true vacuum state as well as the temperature scale. We also need to go into some details of the subsequent evolution of the growth of the bubbles. In particular, we need an estimate of the velocity of the detonation front ζ.

A. Tunneling Rate and Temperature

The decay rate is suppressed by the exponential of the effective action, $\Gamma = \Gamma_0 e^{-S_E(t)}$. The time scale for the decay β given by

$$\beta = -\frac{dS_E}{dt}\Big|_{t=t_*} \tag{19}$$

where t_* is the time when the phase transition occurs. This gives

$$S_E(t) \approx S_E(t_*) - \beta(t - t_*), \tag{20}$$

with the Euclidean action given by

$$S_E = \int d\tau d\vec{x} \left[\frac{1}{2}\left(\frac{d\varphi}{d\tau}\right)^2 + \frac{1}{2}(\vec{\nabla}\varphi)^2 + V(\varphi)\right], \tag{21}$$

where $\tau = it$ is the Euclidean (or Wick rotated) time coordinate. The full, $O(4)$ symmetric solution of Eq. (21) and the nucleation of bubbles was analyzed first by [9, 12] for a universe at zero temperature. At finite temperature T, [13] pointed out that the field theory should be taken periodic in τ with period T^{-1}. Hence Eq. (21) must be written as

$$S_E(t) = \int_0^{1/T} d\tau d\vec{x} \left[\frac{1}{2}\left(\frac{d\varphi}{d\tau}\right)^2 + \frac{1}{2}(\vec{\nabla}\varphi)^2 + V(\varphi, T)\right], \tag{22}$$

where $V(\varphi, T)$ is the temperature dependent effective potential. At sufficiently large temperatures, i.e. when the integrand is approximately time independent over time scales T^{-1}, the integration over τ is reduced simply to the multiplication of T^{-1}, or $S_E = S_3/T$ [14]. Here S_3 has $O(3)$ symmetry and is given by

$$S_3 = 4\pi^2 \int dr \left[\frac{1}{2}(\partial_r\varphi)^2 + V(\varphi, T)\right] \tag{23}$$

$$= 4\pi R(T)^2 S_1(T) - \frac{4}{3}\delta V(T)\pi R(T)^3, \tag{24}$$

where the last equality assumes the thin-wall approximation. $S_1(T)$ is the solution of Eq. (22) to zeroth order in $\delta V(T) = \varepsilon(T)\varphi_1^3\varphi_2^3(\varphi_2^2 - \varphi_1^2)$

$$S_1(T) = \int_{\varphi_1}^{\varphi_2} d\varphi \sqrt{2V(\varphi, T)} \tag{25}$$

$$= \frac{1}{15}\sqrt{\frac{\lambda_3}{2}}(\phi_2 - \phi_1)^3(\phi_1^2 + 3\phi_1\phi_2 + \phi_2^2), \tag{26}$$

which is independent of the temperature as all T dependence is in δV.

The temperature dependent bubble radius

$$R(T) = \frac{2S_1}{\delta V(T)}, \tag{27}$$

is obtained by minimizing S_3. Plugging this back in (24) we find

$$S_3 = \frac{16\pi S_1^3}{3\delta V(T)^2}. \tag{28}$$

Note that for this thin wall approximation to hold, the bubble radius must be much larger than the thickness of the wall, $R \gg (\partial_\varphi^2 V(\varphi))^{-\frac{1}{2}}\Big|_{\varphi=\varphi_2}$. We can now estimate the time scale of the bubble nucleation process β

$$\beta = \frac{16\pi^2}{3}S_1^3\partial_T\frac{1}{\delta V(T)^2 T}$$

$$= \frac{16\pi^2}{3}S_1^3\frac{4cT^2\varphi^2 - \delta V(T)}{T^2\varphi^4\delta V(T)}. \tag{29}$$

The temperature T_* at which the transition takes place is computed in a two step process.

First, we fix ϵ_0 by requiring that the probability is much smaller than unity for our Hubble patch to already have performed the second phase transition during the lifetime of the universe or in other words, by demanding that our Hubble patch is still in the false vacuum at φ_1. Therefore we have

$$t_H^4 H^2 e^{-S} = t^2 e^{-S} \ll 1 \tag{30}$$

which implies

$$S \gg 2\ln\frac{t}{t_P} \approx 280 \equiv S_{\text{crit}}, \tag{31}$$

where t_P is the Planck time. The smallest value of the action, i.e. the highest probability for the transition from $\phi_1 \to \phi_2$ to occur, is realized at zero temperature. Thus we can substitute the action at temperature T by the zero temperature action to obtain a lower limit on the action.

$$S_E(0) = \frac{27\pi^2}{2} \frac{S_1^4}{\delta V(0)^3} \qquad (32)$$

$$= \frac{27\pi^2}{2} \frac{S_1^4}{\epsilon_0^3 (\phi_1^3 \phi_2^3 (\phi_2^2 - \phi_1^2))^3} , \qquad (33)$$

which should be larger than the critical action

$$S_E(0) > S_{\text{crit}} . \qquad (34)$$

This implies

$$\epsilon_0 < \frac{27\pi^2}{2S_{\text{crit}}} \frac{S_1^4}{(\phi_1^3 \phi_2^3 (\phi_2^2 - \phi_1^2))^3} . \qquad (35)$$

Then, we estimate the transition temperature by equating

$$S_E \approx \frac{S_3}{T} , \qquad (36)$$

and solving for T, which should at least give us a rough estimate.

Taking $\varphi_1 = 0.246\text{TeV}$, $\varphi_2 = 0.8\text{TeV}$, $\lambda_3 = 0.154\text{TeV}^{-4}$ and $S_{\text{crit}} = 425$, we find $\varepsilon_0 = 0.15\text{TeV}^{-4}$ and a transition temperature of order $T_* = 0.0128\text{TeV}$.

From the transition temperature we can now determine β/H_*, the quantity of interest (as we shall see in the next section). We first need to make use of the fact that during radiation domination

$$H^2 = \frac{1}{3}\rho = \frac{\pi^2}{90} N(T) T^4 , \qquad (37)$$

$$dt = -\frac{1}{2\pi} \sqrt{\frac{45}{\pi N(T)}} \frac{dT}{T^3} , \qquad (38)$$

where $N(T)$ is the effective number of particles, see e.g. [15] for more details. Thus we have

$$\frac{\beta}{H} = -\frac{1}{H} \frac{\partial S_E}{\partial t} = 2\sqrt{2\pi} T \frac{\partial S_E}{\partial T} \approx 5T \frac{(\partial S_3/T)}{\partial T} \approx 1500 , \qquad (39)$$

c.f. [16] who dropped the numerical prefactor.

B. Growth of Bubbles

In this subsection, we estimate several quantities pertaining to the growth of the bubbles, notably the relativistic γ of the bubble wall.

An expanding bubble of true vacuum behaves very much like a detonation. This was first examined in detail by [17] and the to first order phase transitions by [5].

In a detonation, high temperature gas enters the nucleated bubble with supersonic velocity. This prevents a shock from preceding the bubble wall. The velocity of the detonation front is given by

$$\xi_d = \frac{1/\sqrt{3} + \sqrt{\gamma^2 + 2\gamma/3}}{1 + \gamma} \qquad (40)$$

where the relativistic γ is approximately the ratio of vacuum energy to thermal energy. There are several ways to estimate its value, but they all amount to numbers of the same magnitude.

The efficiency factor, or fraction of latent heat that goes into the kinetic energy rather than thermal energy, is defined as

$$\kappa(\gamma) = \frac{1}{1 + 0.715\gamma} \left[0.715\gamma + \frac{4}{27}\sqrt{\frac{3\gamma}{2}} \right] . \qquad (41)$$

To determine the latent heat and vacuum energy associated with the transition, we begin with the value of the potential at the broken phase minimum which is also the difference in free energy density between the two states of the system. We denote this by

$$B(T) = -V(v(T), T) , \qquad (42)$$

where $v(T)$ is the value of the broken phase minimum. The vacuum energy associated with the transition is then

$$\mathcal{E}_* = B(T) - T B'(T)\big|_{T=T_*} . \qquad (43)$$

This results in a relativistic factor γ of

$$\gamma = \frac{30\mathcal{E}_*}{\pi^2 g_* T_*^4} \sim 11200 . \qquad (44)$$

Alternatively, we could estimate γ just like in [10] to be

$$\gamma = \frac{\rho_{vac}}{T_*^4} \sim 23650 . \qquad (45)$$

Both estimates for γ resultin a very large number. The wall velocity then approaches speed of light, and the efficiency approaches unity

$$\xi_d \approx 1 \approx \kappa . \qquad (46)$$

Hence we are justified in using the approach in Sec. III.

One final remark is in order. In Sec. II we have arbitrarily set $V_0' = 0$. However, the chosen value of V_0' effects the value of the vacuum energy associated with the transition, see Eq. (43). In particular, the presence of a non-zero V_0' acts as a overall shift in the vacuum energy, since the derivative of the potential at the broken minimum, $B'(T)$, is independent of V_0'. Therefore one would write the vacuum energy as $\mathcal{E}_*' = \mathcal{E}_* + V_0'$. However, since γ is so large, the constant shift, which is on the order of a few TeV, would increase the above numbers. But as $\gamma, \xi_d,$, and κ are already indistinguishable from their values in the limit $\gamma \to \infty$, this shift is not important for the determination of the gravitational wave spectrum.

C. Gravitational Wave Spectrum

The spectrum of gravitational waves emitted from bubble collisions was first found by [5]. The fraction of the energy density compared to the critical energy density is given by

$$\Omega_{GW} h^2 \approx 1.1 \times 10^{-6} \kappa^2 \left(\frac{H_*}{\beta}\right)^2$$
$$\times \left(\frac{\gamma}{1+\gamma}\right)^2 \left(\frac{\xi_d^3}{0.24 + \xi_d^3}\right) \left(\frac{100}{g_*}\right)^{1/3} . \quad (47)$$

The maximum of the spectrum is located at

$$f_{max} \approx 5.2 \times 10^{-8} \text{Hz} \left(\frac{\beta}{H_*}\right) \left(\frac{T_*}{1\text{GeV}}\right) \left(\frac{g_*}{100}\right)^{1/6} , \quad (48)$$

and the characteristic amplitude of a gravity wave is approximately

$$h_c(f_{max}) \approx 1.8 \times 10^{-14} \kappa \left(\frac{\gamma}{1+\gamma}\right) \left(\frac{H_*}{\beta}\right)^2$$
$$\times \sqrt{\frac{\xi^3}{0.24 + \xi^3}} \left(\frac{100}{g_*}\right)^{1/3} . \quad (49)$$

In the previous section we found that $\gamma \to \infty$ so that $\xi_d \to 1$ and $\kappa \to 1$. Plugging in these values, we find

$$\Omega_{GW} h^2 \approx 1.1 \times 10^{-6} \left(\frac{H_*}{\beta}\right)^2 \left(\frac{1}{1.24}\right) \left(\frac{100}{g_*}\right)^{1/3} , \quad (50)$$

$$f_{max} \approx 5.2 \times 10^{-8} \text{Hz} \left(\frac{\beta}{H_*}\right) \left(\frac{T_*}{1\text{GeV}}\right) \left(\frac{g_*}{100}\right)^{1/6} , \quad (51)$$

$$h_c(f_{max}) \approx 1.8 \times 10^{-14} \left(\frac{H_*}{\beta}\right)^2 \sqrt{\frac{1}{1.24}} \left(\frac{100}{g_*}\right)^{1/3} . \quad (52)$$

Therefore for bubble collisions we get $\Omega h^2 \approx 1.7 \times 10^{-11}$ and $h_c \approx 3.1 \times 10^{-19}$, peaking at a frequency around $f_{max} \approx 3.5 \times 10^{-4}$ Hz.

We briefly note that for smaller values of $\varepsilon_0 \approx 0.005\text{TeV}^{-4}$, the transition occurs at temperature $T_* \approx 3\text{GeV}$. This gives $\beta/H_* \approx 3.7 \times 10^9$, leading to an amplitude $\Omega_{GW} h^2 \sim 1.1 \times 10^{-25}$ at peak frequency $f_{max} \sim 10^3\text{Hz}$.

V. CONCLUSION

We have considered the standard Higgs field, albeit with a potential containing higher order non-renormalizable terms. Introducing these non-renormalizable terms induced a second minimum in the potential, see Fig. 1. The presence of the first quadratic term in Eq. (8) ensures that the two minima are non-degenerate at sufficiently low temperatures. There is a false-vacuum (a local minimum) and a true-vacuum (a global minimum). In the context of this model we assume that our universe is currently in the false vacuum. The presence of the second lower minimum means that the false-vacuum can decay via the nucleation and expansion of bubbles of true-vacuum from a first-order phase transition. As the bubbles are growing, they will eventually collide with other bubbles, resulting in the production of gravity waves. In this paper we have investigated the gravity wave spectrum from bubble collisions using the envelope approximation developed in [5]. We have also considered the resulting gravity waves from detonating bubbles.

For bubble collision from a given first-order phase transition, knowledge of the model-specific parameters β, ξ, κ and γ suffices to determine the resulting gravity wave spectrum, see Eqs. (47) - (49). The effective potential for bubble nucleation suffices to determine the spectrum of gravitational radiation. Here we find that for the Higgs potential containing the non-renormalizable terms Eq. (2), the transition occurs at a temperature $T_* \approx 12.8\text{GeV}$ (see Section IV A), $\beta/H_* \approx 300$, and $\gamma \sim 10^4$, so that $\xi_d \approx 1 \approx \kappa$ (see Section IV B). Using these results and Eqs. (47) - (49) from Section IV C, we find that the energy density of gravity waves $\Omega h^2 \approx 1.7 \times 10^{-11}$, their characteristic amplitude $h_c \approx 3.1 \times 10^{-19}$, and a peak frequency around $f_{max} \approx 3.5 \times 10^{-4}$ Hz.

The question then arises whether or not the gravity wave signal is potentially detectable by current or future gravity wave experiments. Here we consider some of the possible detectors and their projected sensitivities and compare with our results. First we shall consider a current land-based detector. From [18, 19] the ultimate sensitivity to a background for the Laser Interferometric Gravitational Wave Observatory (LIGO) is an amplitude around 2×10^{-25} at a frequency of 100Hz. However, as we saw in Section IV C, we found that $f_{max} \approx 8.2 \times 10^{-4}\text{Hz}$ with an amplitude of 1.7×10^{-11}, which are well below this requirement. Therefore a detection by LIGO is very unlikely. Next we consider a future space-based experiment. The peak sensitivity for the Laser Interferometer Space Antenna (LISA) [16, 20, 21] is reached in the frequency range between $3 \times 10^{-2}\text{Hz}$ and 10^{-1}Hz with $\Omega_{GW} h^2 \sim 10^{-10}$ - 10^{-12}. From Section IV C we see that our results fall within this range of detection from LISA, hence a detection by LISA could be possible given our results.

One thing to note, however, is that the value of $\varepsilon_0 = 0.15$ TeV^{-4} is an upper limit since smaller values of ε_0 further decrease the bubble nucleation rate. Repeating the calculations above, we see from Eqs. (47) - (49) that as ε_0 decreases, $\Omega_{GW} h^2$ and $h_c(f_{max})$ both decrease while f_{max} increases. For the value of ε_0 given in Fig. 1, $\Omega_{GW} h^2 \sim 3 \times 10^{-18}$ which is well outside the range of LISA. However, as ε_0 falls below 0.005TeV^{-4} the peak frequency and amplitude shift into a window that may

be detectable by LIGO. For this value of ε_0 the transition occurs at temperature $T_* \approx 3\text{GeV}$, $\beta/H_* \approx 3.7 \times 10^9$. This lead to an amplitude of $\Omega_{GW} h^2 \sim 1.1 \times 10^{-25}$ at peak frequency $f_{max} \sim 10^3 \text{Hz}$.

Even though we don't consider these here, additional contributions to the gravity waves spectrum (which could be comparable to, or maybe even stronger than bubble collisions) could come from the period of turbulence after the phase transition, see [22]. First of all, turbulence itself sources gravitational waves. In addition to that, turbulence can also source magnetic fields during the time of the phase transition, see [22, 23]. These induced magnetic field will then act as a source of gravitational radiation until they are damped out. The gravitational radiation from the latter process is subdominant to that of the turbulence, however, its peak frequency is much higher and could potentially be detected at a land-based detector such as LIGO. It would be interesting to investigate the spectrum of gravity waves sourced by these effects as well as the induced magnetic fields.

[1] Eric Greenwood, Evan Halstead, Robert Poltis, and Dejan Stojkovic. Dark energy, the electroweak vacua and collider phenomenology. *Phys. Rev.*, D79:103003, 2009.

[2] J. Abadie et al. All-sky search for gravitational-wave bursts in the first joint LIGO-GEO-Virgo run. *Phys. Rev.*, D81:102001, 2010.

[3] Curt Cutler. Angular resolution of the LISA gravitational wave detector. *Phys. Rev.*, D57:7089–7102, 1998.

[4] Arthur Kosowsky, Michael S. Turner, and Richard Watkins. Gravitational radiation from colliding vacuum bubbles. *Phys. Rev.*, D45:4514–4535, 1992.

[5] Marc Kamionkowski, Arthur Kosowsky, and Michael S. Turner. Gravitational radiation from first order phase transitions. *Phys. Rev.*, D49:2837–2851, 1994.

[6] Christophe Grojean, Geraldine Servant, and James D. Wells. First-order electroweak phase transition in the standard model with a low cutoff. *Phys. Rev.*, D71:036001, 2005.

[7] K. S. Viswanathan and J. H. Yee. FIRST ORDER PHASE TRANSITIONS IN GAUGE THEORIES. *Phys. Rev.*, D19:1906–1911, 1979.

[8] A. Vilenkin and E. P. S. Shellard. *Cosmic Strings and Other Topological Defects*. July 2000.

[9] Sidney R. Coleman. The Fate of the False Vacuum. 1. Semiclassical Theory. *Phys. Rev.*, D15:2929–2936, 1977.

[10] Arthur Kosowsky and Michael S. Turner. Gravitational radiation from colliding vacuum bubbles: envelope approximation to many bubble collisions. *Phys. Rev.*, D47:4372–4391, 1993.

[11] S. Weinberg. *Gravitation and Cosmology*. Cambridge University Press, 1972.

[12] Curtis G. Callan, Jr. and Sidney R. Coleman. The Fate of the False Vacuum. 2. First Quantum Corrections. *Phys. Rev.*, D16:1762–1768, 1977.

[13] Andrei D. Linde. On the Vacuum Instability and the Higgs Meson Mass. *Phys. Lett.*, B70:306, 1977.

[14] Andrei D. Linde. Decay of the False Vacuum at Finite Temperature. *Nucl. Phys.*, B216:421, 1983.

[15] Andrei D. Linde. Elementary particles and inflationary universe: On present formation of theories. (In German). Heidelberg, Germany: Spektrum Akad. Verl. (1993) 304 p.

[16] Riccardo Apreda, Michele Maggiore, Alberto Nicolis, and Antonio Riotto. Gravitational waves from electroweak phase transitions. *Nucl. Phys.*, B631:342–368, 2002.

[17] Paul Joseph Steinhardt. Relativistic detonation waves and bubble growth in false vacuum decay. *Phys. Rev.*, D25:2074, 1982.

[18] K. S. Thorne. Gravitational Radiation. In *Hawking, S.W. (ed.), Israel, W. (ed.): Three hundred years of gravitation*, 330-458. (see Book Index).

[19] Alex Abramovici et al. LIGO: The Laser interferometer gravitational wave observatory. *Science*, 256:325–333, 1992.

[20] C. Delaunay, Christophe Grojean, and G. Servant. The Higgs in the sky: Production of gravitational waves during a first-order phase transition. *AIP Conf. Proc.*, 903:24–31, 2007.

[21] LISA Project. Laser interferometer space antenna (lisa) measurement requirements flowdown guide. Technical report, LISA, April 2009.

[22] Arthur Kosowsky, Andrew Mack, and Tinatin Kahniashvili. Gravitational radiation from cosmological turbulence. *Phys. Rev.*, D66:024030, 2002.

[23] Jarkko Ahonen and Kari Enqvist. Magnetic field generation in first order phase transition bubble collisions. *Phys. Rev.*, D57:664–673, 1998.